Acta Cryst. (1978). A**34**, 242–249

An X-ray Diffuse-Scattering Study of the Ordered, Cubic, $F\bar{4}3m$ Phase of Adamantane (Tricyclo[3.3.1.1^{3,7}]decane)

BY P. A. REYNOLDS

Research School of Chemistry, Australian National University, PO Box 4, Canberra, ACT 2600, Australia

(*Received* 25 *July* 1977; *accepted* 13 *September* 1977)

X-ray diffuse-scattering experiments at 295 and 218 K on adamantane crystals, grown by annealing, show that its space group is $F\bar{4}3m$, and that it is not orientationally disordered. A re-analysis of previous X-ray Bragg-scattering data shows that the conclusion of $Fm3m$, with orientational disorder, for sublimation-grown crystals is not statistically significant. The Bragg intensities are much less sensitive to orientational disorder than the diffuse scattering. The diffuse scattering shows short-range correlation effects interpretable as pairs of neighbouring molecules tending to adopt local configurations characteristic of the low-temperature $P\bar{4}2_1c$ phase, *i.e.* symmetry breaking in $F\bar{4}3m$.

1. Introduction

Many organic crystals appear to have a phase transition from a low-temperature ordered phase to a high-temperature phase in which the molecules are orientationally disordered ('plastic') (Aston, 1963). The high molecular and crystal symmetry of adamantane has made it the subject of many theoretical and experimental studies, listed in Reynolds (1975*a*) and Pertsin & Kitaigorodsky (1976). Most studies assume that the high-temperature cubic phase of adamantane is orientationally disordered, that is with *equal* populations in the two molecular orientations which are related by inversion. The only evidence for this derives from X-ray diffraction (Nordman & Schmitkons, 1965).

In the next section we will summarize the results of the previous work. After developing a simple theory for the diffuse scattering in adamantane we will present our experiments on its X-ray diffuse scattering. These will be fitted to the model to show that a high-temperature cubic phase of adamantane is orientationally ordered. Lastly we will discuss, and reinterpret, the X-ray Bragg-scattering results of Nordman & Schmitkons (1965) (hereinafter N & S) to show that they do *not* necessarily imply a disordered phase.

2. Previous X-ray diffraction work

Photographic data have been taken by N & S on both the low-temperature phase ($P\bar{4}2_1c$, tetragonal, $a = 6{\cdot}60$ $c = 8{\cdot}81$ Å at 160 K) and the high-temperature phase ($F\bar{4}3m$, cubic, $a = 9{\cdot}45$ Å at 295 K) of adamantane. After a subsequent re-refinement of the low-temperature data by Donohue & Goodman (1966), all three space groups were found to give molecules with the same undistorted $\bar{4}3m$ symmetry, in which a reasonable fit is obtained by the use of a single isotropic temperature factor. In the high-temperature cubic phase, introduction of a rigid-body translational and a rigid-body librational thermal factor further improves the fit. The three structures (low-temperature and two alternative high-temperature) are closely related. This is illustrated schematically in Fig. 1. The $F\bar{4}3m$ structure can be obtained from the $Fm3m$ by ordering all the molecules to a similar orientation. $P\bar{4}2_1c$ can be obtained from $Fm3m$ by ordering all the molecules' orientations in alternating ab layers. The molecular orientations in neighbouring ab layers are related by inversion. A subsequent 9° twist around [001], alternating in sign for neighbouring ab layers, and a small tetragonal cell distortion, give the observed $P\bar{4}2_1c$ structure. N & S concluded, on the

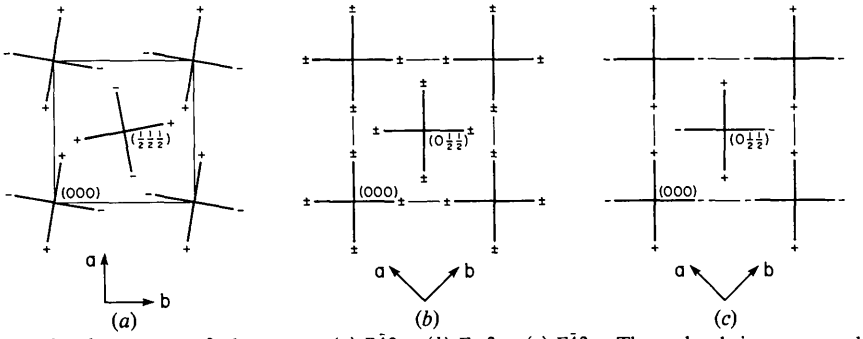

Fig. 1. The three postulated structures of adamantane (*a*) $P\bar{4}2_1c$, (*b*) $Fm3m$, (*c*) $F\bar{4}3m$. The molecule is represented as a tetrahedron.

basis of an analysis which we will discuss later, that the cubic phase is disordered, $Fm3m$.

Moore & Lang (1973) have published a note on the X-ray diffuse scattering from adamantane concluding, without giving any numerical results, that the cubic phase is disordered, $Fm3m$. As we shall see, apart from a (large) intensity scaling factor, both $Fm3m$ and $F\bar{4}3m$ give similar diffuse scattering, differing in detail rather than broad features. Use of polychromatic radiation, short exposure times (Moore, 1975, private communication) and crystals with large, irregular, mosaic spreads could obscure these differences.

3. A simple theory of X-ray scattering in adamantane

We define the space Fourier transform of the molecular electron density as $F_\theta(\mathbf{Q})$, with real and imaginary parts $A_\theta(\mathbf{A})$ and $B_\theta(\mathbf{Q})$. θ represents the rotation of the molecule's twofold axes away from the unit-cell axes. $\mathbf{Q}$ is the total wavevector transfer, $\mathbf{q}$ the position within a Brillouin zone and $\mathbf{h}$ labels the Brillouin zone centre (or Bragg point). Thus

$$\mathbf{Q} = \mathbf{h} + \mathbf{q}. \tag{1}$$

We introduce an order parameter $S_{l,m,n}$, defined in the usual way as $[2p_{l,m,n} - 1]$. $p_{l,m,n}$ is the probability that the molecule separated by a translation $[l,m,n]$ from the reference molecule has the same orientation. For $l,m,n = \infty$, S_{lmn} is the long-range order parameter (S_∞). For $F\bar{4}3m$ $S_\infty = 1$; and for $Fm3m$ $S_\infty = 0$. We will label the nearest-neighbour short-range-order parameter $S_{\frac{1}{2},\frac{1}{2},0}$ as S_1. We will approximate all the S_{lmn} as

$$S_{l,m,n} = S_\infty + (S_1 - S_\infty)^{n+m+l}. \tag{2}$$

We assume that the crystal vibrations, and the order–disorder between the two positions ('**0**' and '**90**'), are mutually independent. We can write the total scattering (I) as a Bragg component (I_B) plus diffuse intensity arising from the order–disorder (I_{DS}), and vibrations (I_{DV}) (Zachariasen, 1945).

$$I = I_B + I_{DS} + I_{DV}. \tag{3}$$

We have neglected the Compton scattering and any background scattering.

If we assume that the translations and librations both contribute to an isotropic thermal factor (β) we can write

$$I_B = [A_0^2(\mathbf{Q}) + S_\infty^2 B_0^2(\mathbf{Q})] \exp(-\beta|\mathbf{Q}|^2)\delta(\mathbf{Q} - \mathbf{h}). \tag{4}$$

The order–disorder component is simplified since in this molecule

$$F_{90}(\mathbf{Q}) = A_0(\mathbf{Q}) - iB_0(\mathbf{Q}) \tag{5}$$

and (2) allows a summation to be made, reflecting the short-range order, to a function $\Gamma_S(\mathbf{q})$ (Flack, 1970).

$$I_{DS} = (1 - S_\infty)^2 B_0^2(\mathbf{Q})\Gamma_S(\mathbf{q}) \exp(-\beta|\mathbf{Q}|^2) \tag{6}$$

where

$$\Gamma_S(\mathbf{q}) = y_x y_y y_z \tag{7}$$

and

$$y_x = [1 - 2(S_1 - S_\infty)\cos \pi q_x + (S_1 - S_\infty)^2]^{-1}. \tag{8}$$

We can approximate the one-phonon contribution from the translations and librations by taking the $|\mathbf{Q}|^2$ dependent term in the relation $I = |\bar{F}|^2 - |\overline{F^2}|$, where the averages are taken over the thermal motion.

This gives

$$I_{DV} = F_0(\mathbf{Q})F_0^*(\mathbf{Q})\beta|\mathbf{Q}|^2\Gamma_V(\mathbf{q}) \exp(-\beta|\mathbf{Q}|^2) \tag{9}$$

where $\Gamma_V(\mathbf{q})$ is an arbitrary function introduced to take some account of the dispersion of an 'average' phonon. For undispersed phonons $\Gamma_V(\mathbf{q}) = 1$. We would expect this formula to fail badly near $\mathbf{q} = 0$, at allowed Bragg reflections, because of the acoustic phonons. Multi-phonon scattering becomes important when $\beta|\mathbf{Q}|^2 \gtrsim 1$. For the librational component the dynamical structure factor is simplified if we regard the librational amplitude as small. Then we can put $\bar{F} \cong F_0(\mathbf{Q})$. We must further assume an *isotropic* thermal factor resulting from the librations, which is a more drastic approximation than for the translations.

We can now model the experimental X-ray intensity of the cubic phase of adamantane. We must assume a molecular geometry and then fit six parameters, β, $\Gamma_V(\mathbf{q})$, $\Gamma_S(\mathbf{q})$, S_∞, S_1, and a normalizing factor. From the Bragg scattering we can in principle obtain the thermal factor β and S_∞, the long-range-order parameter. β is well determined by a rigid-body refinement, but S_∞ is not. This is because for adamantane $A_\theta(\mathbf{Q}) > B_\theta(\mathbf{Q})$; or qualitatively, for this globular molecule, the scattering is relatively insensitive to the molecular orientation.

However, in the diffuse scattering, S_∞ is determinable if $I_{DS} > I_{DV}$. This will occur if $B_\theta^2(\mathbf{Q}) > A_\theta^2(\mathbf{Q})\beta|\mathbf{Q}|^2$. Since β is small, at low angles of scattering (low $\mathbf{Q}$) this can be ensured. S_∞ is much more easily determined from the diffuse scattering than the Bragg scattering. The accuracy of the other quantities $\Gamma_V(\mathbf{q})$ and S_1 will be lower since the approximations involved in deriving I_{DV} are more drastic than those used in deriving I_{DS}. Use of a more accurate model for the phonon scattering (see, for example, Weulersse, 1970) would involve many more parameters.

At those points where $B_\theta(\mathbf{Q})$ is large $A_\theta(\mathbf{Q})$ is also large, so we expect large phonon diffuse scattering in precisely those regions where any order–disorder scattering is expected to be manifest. Thus, to extract S_∞ one must measure relative intensities either of Bragg-to-diffuse, or of diffuse-to-diffuse at very different $|\mathbf{Q}|$'s. The intensity of order–disorder scattering will also be expected to be less sensitive to temperature than the phonon scattering.

4. Experimental

To measure the X-ray diffuse scattering from adamantane it is necessary to have a large crystal with a volume of several times 0·1 mm^3. This ensures that the background from air scattering is not too large. It is also necessary to enclose the crystal, to prevent sublimation losses, in a material which must not itself scatter significantly more than the air in the beam. Adamantane crystals are extremely plastic and susceptible to mechanical damage. Our crystals were grown by sealing adamantane powder (Aldrich, gold label, 99+%), purified by resublimation, in 0·8 mm diameter Lindemann-glass tubes, with walls of thickness ~0·02 mm. These tubes were annealed for 4 d at a temperature of approximately 510 K. The results were clear cylindrical crystals of 0·8 mm diameter. The crystal mosaic spread was typically less than 1·5° about any axis perpendicular to the tube axis. The mosaic spread around the tube axis was larger. The best crystal had a mosaic spread (full width at $\frac{1}{10}$ maximum) of 6°, with no apparent structure within it. There were no noticeable sublimation losses in six months.

The diffuse scattering was measured with Cu $K\alpha$ radiation (Philips generator 40 kV, 20 mA) monochromated by reflection from a graphite crystal. We used a standard Stoe Weissenberg camera with modified beam stop.

The crystal was face-centred cubic with unit-cell length $a = 9{\cdot}43 \pm 0{\cdot}03$ Å. This agrees with previous values of 9·54 (Giacomello & Illuminati, 1945), $9{\cdot}426 \pm 0{\cdot}008$ (Nowacki, 1945) and 9·45 (N & S).

The intensities of the Bragg peaks were measured visually from a 180° rotation photograph about [001] (Fig. 2). Rotation automatically integrates, approximately, over the large mosaic spread around the tube axis. At the end of the diffuse-scattering measurements, rotation photographs were made at 300, 170 and 300 K successively, with a Stoe low-temperature attachment used to observe the phase change to the low-temperature $P\bar{4}2_1c$ phase. The diffuse scattering was sampled by use of Laue photographs with up to 4 h exposure at 295 and 218 K (Fig. 3). There were eight intense lobes at 2·2, 2·2, 2·2 with six less intense maxima at 550. There appears to be more detailed structure. This was examined at 295 K by taking Weissenberg photographs of $hk\frac{1}{2}$, $hk\frac{3}{2}$, $hk\frac{5}{2}$ (Figs. 4, 5). Maximum resolution consistent with the crystal size was obtained by using 0·8 mm separation between the screens. 48 h exposures were taken. Intensities were measured with a Joyce–Loebl microdensitometer.

5. Discussion and fit of diffuse scattering data

(*a*) *Qualitative features*

The eight intense lobes of diffuse scattering near the symmetry-related points 2·2, 2·2, 2·2 correspond

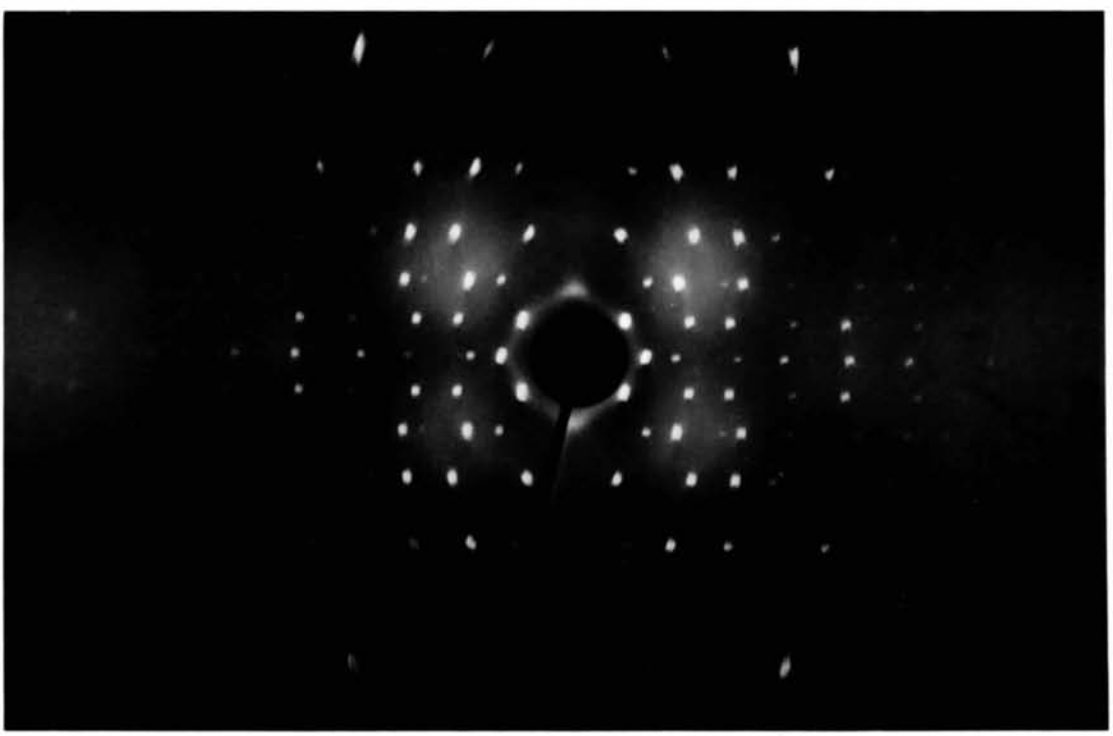

Fig. 2. Adamantane, 180° rotation photograph about [001].

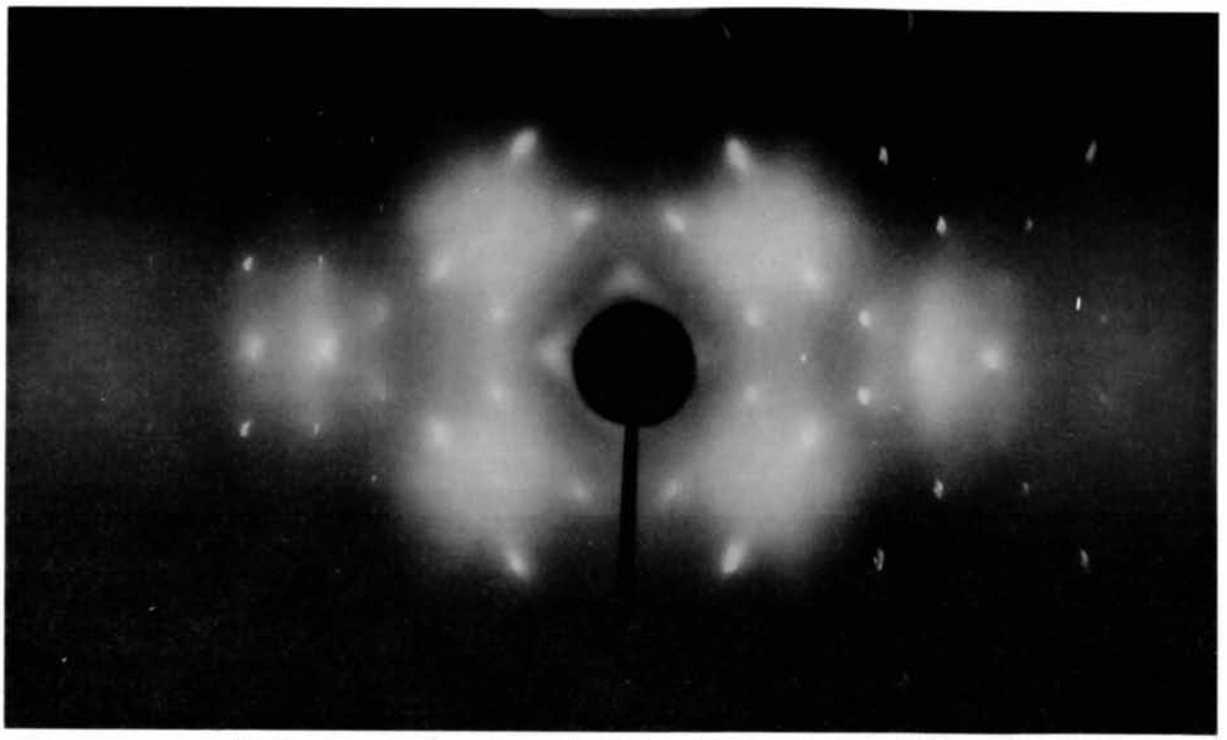

Fig. 3. Adamantane, Laue photograph, [010] parallel to incoming beam, [100] vertical.

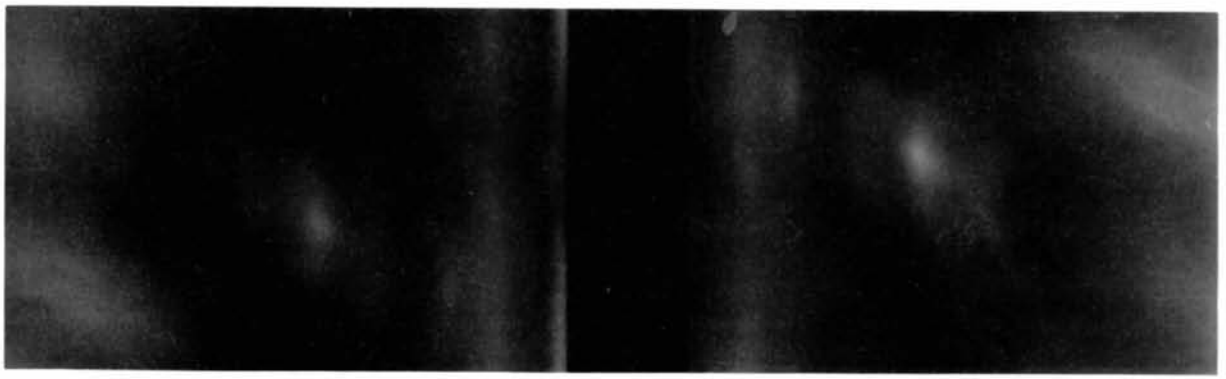

Fig. 4. Adamantane, Weissenberg photograph of $hk\frac{1}{2}$ layer.

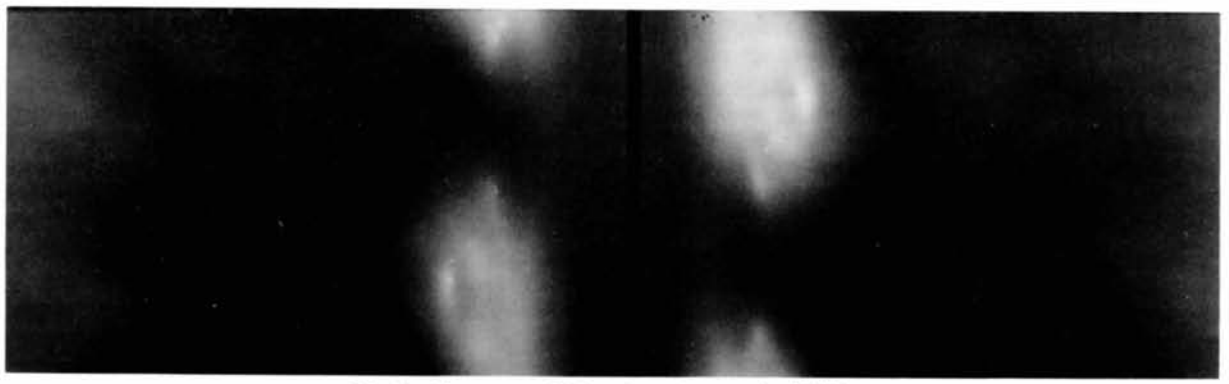

Fig. 5. Adamantane, Weissenberg photograph of $hk\frac{3}{2}$ layer.

with points at which both the real [$A_0(\mathbf{Q})$] and imaginary [$B_0(\mathbf{Q})$] parts of the Fourier transform of the molecular electron density are at their maximum values. Similarly, near the points 550 there are also maxima in both $A_0(\mathbf{Q})$ and $B_0(\mathbf{Q})$ corresponding to intense X-ray diffuse scattering. A cursory inspection is therefore unable to distinguish between $F\bar{4}3m$ (in which the observed scattering, I_o, is proportional to $|\mathbf{Q}|^2A_0^2(\mathbf{Q})$ and $Fm3m$ [where $I_o \propto B_0^2(\mathbf{Q})$]. The Laue photographs showed that, in the most intense lobes at 2·2, 2·2, 2·2, the intensity was modulated such that intensities near the Brillouin zone centres [$\mathbf{q} = (000)$] were greater than at $\mathbf{q} = (\frac{111}{222})$, $(00\frac{1}{2})$ or $(\frac{11}{22}0)$. This 'heaping up' of diffuse intensity occurred at all the Bragg points including those where the Bragg scattering was forbidden in this F-centred lattice. We note that extra scattering, due to acoustic modes, was not obviously present even near Bragg points with strong Bragg scattering for $|\mathbf{q}| > 0{\cdot}1$. In the Weissenberg photographs (Fig. 4) the diffuse intensity is modulated into festoons along [$hh0$], such that the intensity along [$h\bar{h}0$] varies slowly while that along [$hh0$] varies more quickly. We note, however, that the effect of the 6° mosaic spread about the tube (=rotation) axis is to smear any possible short-range intensity modulation along these festoons. The effect of the mosaic spread on the experimental resolution is least along [$hh0$]. By measurement along this direction we may obtain an approximate measure of $[\Gamma_n(00\frac{1}{2})/\Gamma_n(\frac{111}{222})]$, where n depends on the mechanism by which the intensity arises (vibrations or disorder).

(*b*) *Intensity of diffuse scattering relative to Bragg scattering*

We measured the intensity of the diffuse scattering at 2, 2, 2·5, where it is almost at its most intense, relative to the weak Bragg peaks 048, 068, 026, 137, 226 and 244. The resolution function was such that $\sim\frac{1}{200}$ of the Brillouin zone volume was covered by a Bragg spot. We assume values of $\beta = 0{\cdot}022$, derived from N & S's refinement of the Bragg scattering. The structure factor of 024 ($F_{024} \cong 1{\cdot}4$) varies little between experiment and either of the refinements in $F\bar{4}3m$ and $Fm3m$. We therefore use this reflection to obtain values of the structure factors at other places. We obtain (N & S's values in brackets) $F_{222\frac{1}{2}} = 3{\cdot}9 \pm 1{\cdot}0$. $F_{048} = 0{\cdot}5 \pm 0{\cdot}15$ (<0·93), $F_{068} = 0{\cdot}3 \pm 0{\cdot}1$ (<0·61), $F_{026} = 1{\cdot}1 \pm 0{\cdot}3$ (0·65), $F_{137} < 0{\cdot}6$ $F_{226} = 0{\cdot}7 \pm 0{\cdot}2$ (0·60), $F_{244} = 1{\cdot}9 \pm 0{\cdot}3$ (0·63). We will discuss the Bragg intensities in a subsequent section together with those of N & S. Having obtained an absolute value of the structure factor of the diffuse scattering at $2,2,2\frac{1}{2}$ we may use (6) and (9) to obtain a value of $(1 - S_\infty)^2\Gamma_S(00\frac{1}{2})$, a measure of the long-range order. We will assume $\Gamma_V(00\frac{1}{2}) = 1$. We obtain $(1 - S_\infty)^2\Gamma_S(00\frac{1}{2}) = -|0{\cdot}05^{+0.17}_{-0.12}$. Most of the uncertainty arises from the resolution correction used to obtain $F_{2,2,2\frac{1}{2}}$; very little arises from the assumption made for Γ_V. Since it must be positive, we can say $(1 - S_\infty)^2\Gamma_S(00\frac{1}{2})$ is less than 0·12 with a preferred value of 0. For the $F\bar{4}3m$ structure we expect a value of 0; and for $Fm3m$ of slighly less than 1. If $(1 - S_\infty)^2\Gamma_S(00\frac{1}{2})$ were unity this would raise the observed diffuse intensity by a factor of four relative to the Bragg peaks. This illustrates the sensitivity of the diffuse scattering to the disorder.

(*c*) *Relative intensities of diffuse scattering at* 295 K

We can exploit the different $|\mathbf{Q}|$ dependence of disorder and one-phonon scattering to obtain another, independent, estimate of $(1 - S_\infty)^2\Gamma_S(\mathbf{q})$. We have measured the diffuse intensity (I_o) for integral and half-integral values of n, along $[nn\frac{1}{2}]$ and $[nn\frac{3}{2}]$. To minimize interference from multiphonon scattering we have neglected points with $\beta|\mathbf{Q}|^2 \gtrsim 1$.

Consideration of (6) and (9) shows that we may hope to extract from these intensities, besides a normalizing constant, $(1 - S_\infty)^2\Gamma_S(nn\frac{1}{2})$ and $\beta\Gamma_V(nn\frac{1}{2})$. The fits to the data of an $F\bar{4}3m$ and an $Fm3m$ model are shown in Table 1. The relative R factors ($R = \Sigma|(I_o - I_c)|/\Sigma I_o$) are 0·16 for the $F\bar{4}3m$ and 0·31 for the $Fm3m$ structures. The best fit, measured by R, is near the $F\bar{4}3m$ structure with $(1 - S_\infty)^2\Gamma_S(00\frac{1}{2}) = (1 -$

Table 1. *Observed and calculated diffuse scattering*

$R(F\bar{4}3m)$ is a normalized ratio of calculated diffuse scattering intensity to $(I_o - 1)$; we have assumed a flat, unit background.

Q	I_o	$R(F\bar{4}3m)$	$R(Fm3m)$
$2\ 2\ \frac{1}{2}$	4·8	0·692	1·24
$2\frac{1}{2}\ 2\frac{1}{2}\ \frac{1}{2}$	4·6	0·866	0·848
$3\ 3\ \frac{1}{2}$	4·9	0·601	0·375
$3\frac{1}{2}\ 3\frac{1}{2}\ \frac{1}{2}$	2·4	0·182	0·213
$4\ 4\ \frac{1}{2}$	2·6	0·812	0·567
$4\frac{1}{2}\ 4\frac{1}{2}\ \frac{1}{2}$	3·5	1·37	0·755
$5\ 5\ \frac{1}{2}$	8·0	0·681	0·400
$5\frac{1}{2}\ 5\frac{1}{2}\ \frac{1}{2}$	4·4	1·07	0·583
$6\ 6\ \frac{1}{2}$	3·3	0·690	0·515
$6\frac{1}{2}\ 6\frac{1}{2}\ \frac{1}{2}$	1·2	*	*
$7\ 7\ \frac{1}{2}$	1·8	*	*
$7\frac{1}{2}\ 7\frac{1}{2}\ \frac{1}{2}$	3·3	*	*
$8\ 8\ \frac{1}{2}$	4·8	*	*
$\frac{1}{2}\ \frac{1}{2}\ 2\frac{1}{2}$	4·4	1·123	1·27
$1\ 1\ 2\frac{1}{2}$	7·0	1·02	2·13
$1\frac{1}{2}\ 1\frac{1}{2}\ 2\frac{1}{2}$	10·1	1·021	2·18
$2\ 2\ 2\frac{1}{2}$	11·6	2·46	2·09
$2\frac{1}{2}\ 2\frac{1}{2}\ 2\frac{1}{2}$	11·7	1·364	1·15
$3\ 3\ 2\frac{1}{2}$	13·0	1·05	0·70
$3\frac{1}{2}\ 3\frac{1}{2}\ 3\frac{1}{2}$	5·8	*	*
$4\ 4\ 2\frac{1}{2}$	2·8	*	*
$4\frac{1}{2}\ 4\frac{1}{2}\ 2\frac{1}{2}$	1·4	*	*
$5\ 5\ 2\frac{1}{2}$	1·8	*	*
$5\frac{1}{2}\ 5\frac{1}{2}\ 2\frac{1}{2}$	1·3	*	*
$6\ 6\ 2\frac{1}{2}$	0·8	*	*

* Intensity neglected in the fit because of appreciable multiphonon scattering.

$S_\infty)^2\Gamma_S(\frac{111}{222}) = 0{\cdot}03 \pm 0{\cdot}05$ and $\Gamma_V(\frac{111}{222})/\Gamma_V(00\frac{1}{2}) = 0{\cdot}6 \pm 0{\cdot}2$. A better statistical analysis is not warranted because of the serious approximations made in deriving the phonon scattering. The values of $(1 - S_\infty)^2\Gamma_S(nn\frac{1}{2})$ are so well determined because at low $|\mathbf{Q}|^2$'s the lack of disorder intensity is very marked. At much higher $|\mathbf{Q}|^2$, when $\beta|\mathbf{Q}|^2 > 1$, the observed intensity is much larger than that calculated – presumably because of the effects of extra multiphonon scattering (proportional to $|\mathbf{Q}|^4$ and higher powers).

To determine the values of the long-range-order parameter (S_∞) and the nearest-neighbour-order parameter (S_1) separately, more information is needed. We can, however, place some limits on the allowed values of S_1 and S_∞, since $0 \leq S_\infty \leq 1$ and $S_1 > S_\infty$. This gives $S_1 \gtrsim 0{\cdot}7$ and $S_\infty \gtrsim 0{\cdot}7$. These limits are compatible with the observation $I_o(|\mathbf{q}| > 0{\cdot}1) \leq I_o(2{\cdot}2,2{\cdot}2,2{\cdot}2)$ which itself provides an estimate of S_1. Any diffuse intensity associated with disorder, if it exists significantly, has a f.w.h.m. of less than 0·2 in the Brillouin zone. This, with (7) and (8), gives $0{\cdot}85 < S_1 \leq 1{\cdot}0$, and therefore $S_\infty > 0{\cdot}85$.

(d) Temperature dependence of diffuse scattering

The Laue photographs taken at 218 K, 10 K above the phase-transition temperature of 208 K, are qualitatively very similar to those at 295 K. Analysis of some intensities at symmetry points around 222 showed that the scattering remains interpretable in terms of one-phonon scattering with no contribution from disorder ($I_{DS} = 0$). We obtain β at 218 K of 0·017 compared with 0·022 at room temperature. This 25% decrease in diffuse scattering intensity, relative to Bragg scattering, contrasts with the very slight increase in intensity expected from disorder scattering due to a decreased Debye–Waller factor. From the Laue photographs we measure $\Gamma_V(\frac{111}{222})/\Gamma_V(00\frac{1}{2})$ of $0{\cdot}70 \pm 0{\cdot}10$ at 295 and $0{\cdot}65 \pm 0{\cdot}10$ at 218 K. This corresponds to the value obtained from the Weissenberg photographs.

6. Bragg-scattering data

Examination of the total intensity within about 0·1 of the allowed Bragg points, which is our resolution, and

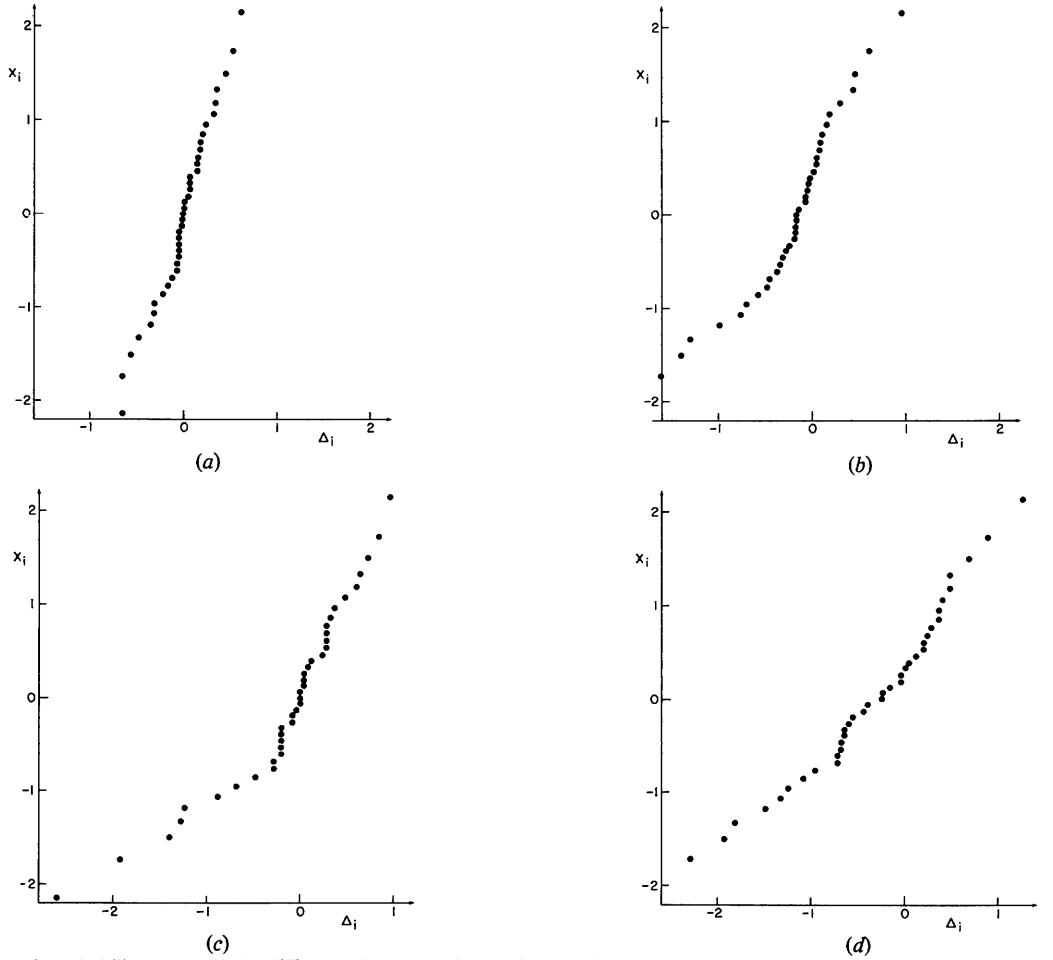

Fig. 6. Normal probability plots of the difference between observed and calculated structure factors, N & S data. (*a*) unweighted data $Fm3m$, (*b*) unweighted data $F\bar{4}3m$, (*c*) weighted data $Fm3m$, (*d*) weighted data $F\bar{4}3m$.

presumably that of N & S too, will allow us to test if the molecules are indeed in ordered clusters of at least 300 molecules (which we will idealize to $F\bar{4}3m$) rather than locally disordered ($Fm3m$). The cluster size arises because if $S_1 > 0{\cdot}85$ then the diffuse intensity will be included under the Bragg peak at our resolution. N & S obtained intensities from 39 independent reflections to which they fitted both $F\bar{4}3m$ and $Fm3m$ models (five variable parameters: scale factor, two carbon coordinates, two thermal parameters). The structure was refined with unweighted structure factors ($\omega_i = 1$). They obtained weighted R factors (Hamilton, 1969), $R = [\Sigma_i \omega_i(|F_o^i| - |F_c^i|^2/\Sigma_i \omega_i|F_o^i|^2]^{1/2}$, of 0·168 for the $F43m$ structure and 0·097 for the disordered $Fm3m$ structure. The ratio of R factors is highly significant providing that $\omega_i = 1$ reflects the true inverse of the variances of the observations. This may be tested in two ways. Firstly, we have an experimental estimate of the variances by use of our independently derived structure factors. Secondly, the residual errors, $\Delta_i = (|F_i(\text{obs})| - |F_i(\text{calc})|)\omega_i^{1/2}$, must be normally distributed. If this is so, *and* if the two models are adequate for modelling an exact set of data to a far greater accuracy than our observed errors, then we may assign significance to R-factor ratios (Hamilton, 1969).

In fact, normal probability plots of Δ_i with $\omega_i = 1$ (Fig. 6*a*,*b*) show markedly curved plots with slopes very far from unity. We can therefore place no reliance on the observed R-factor ratio. It is well known that unweighted data is inadequate, so we have used the weighting scheme of Hughes (1941) and reoptimized the data. We put $\omega_i = 16$ if $F_i(\text{obs}) < 2$ and $\omega_i = 64/F_i^2(\text{obs})$ if $F_i(\text{obs}) \geq 2$. The probability plots obtained are shown in Fig. 6(*c*) and (*d*). These show a relatively straight line for $F\bar{4}3m$ but still a curved line for $Fm3m$. The respective R values are 0·29 and 0·17. Again, because of plot curvature we can make no reasonable choice between the data. This weighting scheme implies a variance of $F^2/64$ in the observed stronger structure factors, *i.e.* an accuracy of intensity measurement of about 25%. In a structure factor of ~1 the accuracy implied is greater. One would therefore expect an R' factor defined as

$$\left|\frac{\Sigma\{\omega_i[|F_i(\text{obs 1})| - |F_i(\text{obs 2})|]^2\}}{\Sigma\,\omega_i|F_i(\text{obs 1})|^2}\right|^{1/2}$$

to be about 0·25. This means that refinement past an R value of about 0·25 is meaningless. The differences in the R values of $F\bar{4}3m$ and $Fm3m$ seem to arise solely because of the chance distribution of measured intensities. We can see that our estimated variances are of the right order by comparing N & S's data and ours, for the independently measured structure factors (§ 5*b*). The discrepancy is even larger than $R' \sim 0{\cdot}25$ would imply since we have measured precisely those intensities calculated to be most different in $Fm3m$ and $F\bar{4}3m$ models.

N & S used a second argument for the $Fm3m$ structure. From (4) we can see that if our $F\bar{4}3m$ model differs from the correct structure only by a change in S_∞ then

$$\frac{F_o}{F_c(\bar{4}3m)} \simeq \left|\frac{A_0^{2\text{calc}}(\mathbf{Q}) + S_\infty^2 B_0^{2\text{calc}}(\mathbf{Q})}{A_0^{2\text{calc}}(\mathbf{Q}) + B_0^{2\text{calc}}(\mathbf{Q})}\right|^{1/2} \qquad (10)$$

the phase angle, α, is given by

$$|\cos\alpha|^2 = A_0^{2\text{calc}}(\mathbf{Q})/[A_0^{2\text{calc}}(\mathbf{Q}) + B_0^{2\text{calc}}(\mathbf{Q})]. \qquad (11)$$

Therefore,

$$\frac{F_o}{F_c(\bar{4}3m)} \simeq [\cos^2\alpha + S_\infty^2(1 - |\cos\alpha|^2)]^{1/2}. \qquad (12)$$

If we plot $F_o/F_c(\bar{4}3m)$ *versus* $|\cos\alpha|$ we can fit a value for S_∞ directly. N & S data give a least-squares value of $S_\infty = 0{\cdot}6 \pm 0{\cdot}4$ for the unweighted data and $S_\infty = 0{\cdot}8 \pm 0{\cdot}4$ for the weighted data. Addition of our measured structure factors to N & S's set increases S_∞ still further towards unity. This method of obtaining S_∞ reveals a preference for $S_\infty = 1$ rather than 0, but there is little significance in the choice because of the large errors. This underlines the inadequacy of Bragg data, measured at this accuracy, in distinguishing between $Fm3m$ and $F\bar{4}3m$ structures. The measured Bragg scattering, because of the experimental finite resolution does not of course really reveal S_∞, since some diffuse intensity is included under the Bragg peak, but an integral of S_∞ and $\Gamma_S(q)$, as do our diffuse scattering measurements.

7. Discussion

(*a*) *Long-range order in molecular orientations differing by* 90°

We will discuss the long-range order (S_∞) in terms of infinite crystals of a disordered $Fm3m$ ($S_\infty = 0$) and an ordered $F\bar{4}3m$ structure ($S_\infty = 1$). From our diffuse scattering measurements of the relative intensity of diffuse and Bragg peaks, the distribution of diffuse intensity and its temperature dependence we find a minimum value for S_∞ of 0·7. The value of this minimum arises from the assumed structure of the short-range ordering (equation 2). Within this theoretical framework it is not possible to fit our results to long-range disorder ($S_\infty = 0$) compensated by much higher short-range order (S_1). Even were it so the value of S_1 ($\gtrsim 0{\cdot}85$) implies ordered clusters of at least 300 molecules [$\sim(1 - S_1)^{-3}$]. These large clusters in an $Fm3m$ structure could only be distinguished from an infinite $F\bar{4}3m$ crystal by examining, at higher resolution, the width of the Bragg peak. For small crystallites of $F\bar{4}3m$, of the order of the cluster size, this distinction between the two alternatives disappears. In the previous section we have shown that the Bragg scattering data of N & S is incapable of distinguishing between the two extreme alternatives ($S_\infty = 1$, $S_1 = 1$ and $S_\infty = 0$, $S_1 = 0$).

The crystals grown by annealing transform to the same $P\bar{4}2_1c$ structure observed on cooling sublimation-grown crystals, and re-attain the ordered $F\bar{4}3m$ structure on warming. It is not impossible that sublimation-grown crystals are of $Fm3m$ long-range symmetry. Cases are known, *e.g.* CCl_4, of production of metastable phases by different crystal-growth techniques (Badiali, Bruneaux-Poulle & Defrain, 1976). The reversibility of the $F\bar{4}3m$ to $P\bar{4}2_1c$ change suggests that any possible $Fm3m$ crystals are metastable with respect to the $F\bar{4}3m$ structure. We should emphasize that $Fm3m$ is the limiting case of $F\bar{4}3m$, with crystallite size reduced to intermolecular dimensions.

(*b*) *Short-range ordering in molecular vibrations*

The one-phonon diffuse scattering is modulated such that intensity is heaped up at the Brillouin zone centre [$\mathbf{q} = (000)$]. A possible interpretation of this is in a local ordering to a structure resembling that of the $P\bar{4}2_1c$ phase. This involves a softening of $F\bar{4}3m$ symmetry-breaking modes at $\mathbf{q} \cong \{000\}$ so that alternate *ab* layers can assume their $P\bar{4}2_1c$ molecular orientations and relative spacings. The size of the local 'clusters' can be estimated from $\Gamma_V(\frac{111}{222})/\Gamma_V(00\frac{1}{2})$ by regarding the process not as mode-softening in a displacive transition, but local ordering in an Ising transition in all coordinates. We estimate the cluster size at room temperature, 100 K above the transition, as about 1·6 molecules. If the ordering occurs in only some of the translations and librations of $\mathbf{q} \sim \{000\}$, the corresponding cluster size is larger. The cluster size is only weakly dependent on temperature. At 218 K it has increased to 1·8 molecules. For such small cluster sizes it may be more useful to regard the correlation as between independent pairs of molecules separated by $[\frac{11}{22}0]$. This would cause a modulation of the diffuse scattering associated with a single molecule into sets of diffuse planes $\{hh0\}$ $h = 1, 2, \ldots, n$. The large mosaic spread of our crystal precludes any more detailed analysis of our data, which would also require a more accurate theoretical treatment of the phonon scattering. An inelastic neutron scattering experiment will be able to distinguish more clearly between the Ising or displacive nature of the transition (Schneider & Stoll, 1976) and determine which modes are involved.

(*c*) *Relation to theories of order–disorder transitions*

Previous theories of the phase transition in adamantane have assumed that the upper phase is orientationally disordered. Ising models then give a good agreement with a number of properties (Reynolds, 1975*a*; Pertsin & Kitaigorodsky 1976) – notably the predicted transition temperature, and specific-heat data. This may not be coincidental, since a similar picture is emerging for 1,4-diazabicyclooctane (Reynolds, to be published). We can postulate a similar situation to that occurring in p-$C_6H_2Cl_2$ (Reynolds, 1975*b*). We can trace a continuous pathway, in order parameters, from an initially ordered phase ($P\bar{4}2_1c$) to a completely disordered phase ($Fm3m$) which reorders to an ordered phase ($F\bar{4}3m$) as the temperature is raised. Much of this pathway may not physically exist, because of lattice expansion. In particular, the $Fm3m$ phase may exist only as a metastable intermediate – at any temperature above T_c it may recorder, *i.e.* increase the crystallite size from 1 to ∞ and expand its volume, to $F\bar{4}3m$: below T_c it may reorder and contract to $P\bar{4}2_1c$. However, the calculated transitional quantities $P\bar{4}2_1c \leftrightarrow$ '$Fm3m$' may resemble those $P\bar{4}2_1c \leftrightarrow F\bar{4}3m$, providing that those for '$Fm3m$' $\leftrightarrow F\bar{4}3m$ are small. This situation is known to be so for the possibly analogous phases of CCl_4 (Morrison & Richards, 1976). The increase in disorder (whether displacive, Ising or intermediate), as we approach T_c from either direction may well mimic other data (such as specific heats) calculated on the basis of an order–disorder transition, provided that the energy quantities involved are similar. In particular the specific heat of adamantane above T_c includes a component that a clustering of molecular 0–90° orientations in a disordered lattice will explain. However, the data will fit equally well *any* other Ising-like process – such as the translational–librational ordering we have postulated in the $F\bar{4}3m$ phase.

References

ASTON, J. G. (1963). *Physics and Chemistry of the Organic Solid State*, edited by D. FOX, M. M. LABES, & A. WEISSBERGER, Vol. 1, pp. 543–582. New York: John Wiley.

BADIALI, J. P., BRUNEAUX-POULLE, J. & DEFRAIN, A. (1976). *J. Chim. Phys. Phys. Chim. Biol.* **73**, 113–115.

DONOHUE, J. & GOODMAN, S. H. (1966). *Acta Cryst.* **22**, 352–354.

FLACK, H. D. (1970). *Philos. Trans. R. Soc. London, Ser. A*, **266**, 561–591.

GIACOMELLO, G. & ILLUMINATI, G. (1945). *Gazz. Chim. Ital.* **75**, 246–256.

HAMILTON, W. C. (1969). *International Tables for X-ray Crystallography*, Vol. 4, § 4.2. Birmingham: Kynoch Press.

HUGHES, E. W. (1941). *J. Am. Chem. Soc.* **63**, 1737–1752.

MOORE, M. & LANG, A. R. (1973). *Proc. Eur. Crystallogr. Meet.*, Bordeaux.

MORRISON, J. A. & RICHARDS, E. L. (1976). *J. Chem. Thermodyn.* **8**, 1033–1038.

NORDMAN, C. E. & SCHMITKONS, D. L. (1965). *Acta Cryst.* **18**, 764–767.

NOWACKI, W. (1945). *Helv. Chim. Acta*, **28**, 1233–1242.

PERTSIN, A. J. & KITAIGORODSKY, A. I. (1976). *Mol. Phys.* **32**, 1781–1784.

REYNOLDS, P. A. (1975*a*). *Mol. Phys.* **30**, 1165–1180.

REYNOLDS, P. A. (1975*b*). *Mol. Phys.* **29**, 519–529.

SCHNEIDER, T. & STOLL, E. (1976). *Phys. Rev. B*, **13**, 1216–1237, and references therein.

WEULERSSE, P. (1970). *Acta Cryst.* A**26**, 628–635.

ZACHARIASEN, W. H. (1945). *Theory of X-ray Diffraction in Crystals*. New York: John Wiley.